J. Aerosol Sci., Vol. 20, No. 3, pp. 367–380, 1989.
Printed in Great Britain.

0021-8502/89 $3.00+0.00

A NUMERICAL STUDY OF INERTIAL ERRORS IN ANISOKINETIC SAMPLING

B. Y. H. Liu, Z. Q. Zhang and T. H. Kuehn

Particle Technology Laboratory, Department of Mechanical Engineering, University of Minnesota, Minneapolis, MN 55455, U.S.A.

(*Received* 4 *August* 1988; *and in final form* 27 *October* 1988)

Abstract—A numerical study has been made of the anisokinetic sampling of aerosols from a flowing gas stream by a thin-walled tube. The sampling error due to anisokinetic sampling conditions has been calculated for various ratios of the free stream gas velocity, W, to the mean gas velocity, V, in the sampling tube. The performance of the sampling inlet is characterized by an aspiration coefficient, A, a penetration coefficient, P, and a loss coefficient, L. The values of A, P, and L have been calculated numerically and correlated with the Stokes number and the velocity ratio by means of simple equations. The numerical results for the aspiration coefficient have been found to be in good agreement with the classical study of Belyaev and Levin [*J. Aerosol Sci.* **3**, 127 (1972); **5**, 325 (1974)] in the velocity ratio, W/V, range of 0.2–5. Outside this range, some discrepancies were found and the classical Belyaev and Levin's results gave increasingly less accurate results.

NOMENCLATURE

A Aspiration coefficient
C Slip correction
C_D Drag coefficient
D_p Particle diameter
d' Diameter of stream tube defined by the limiting trajectory of particles being aspirated into sampling tube
d'' Diameter of stream tube defined by the limiting trajectory of particles penetrating through sampling tube
d_i Inner diameter of the sampling tube
d_o Outer diameter of the sampling tube
F_{dr} Fluid drag on particle in the radial direction
F_{dz} Fluid drag on particle in the axial direction
L Loss coefficient
P Penetration coefficient
R Radius of the cylindrical calculation domain
R_i Inner radius of the sampling tube
R_o Outer radius of the sampling tube
Re Reynolds number of the sampling tube $=\dfrac{\rho d_i W}{\mu}$
Re_p Local particle Reynolds number $=\mathrm{Re}_{p'w}[(u'_r-v'_r)^2+(u'_z-v'_z)^2]^{1/2}$
$\mathrm{Re}_{p'w}$ Mean particle Reynolds number $=\dfrac{\rho D_p W}{\mu}$
St Stokes number $=\dfrac{\tau W}{d_i}$
u_r, u_z Radial and axial components of the fluid velocity
v_r, v_z Radial and axial components of the particle velocity
u'_r, u'_z Dimensionless fluid velocity $=u_r/W$, u_z/W
v'_r, v'_z Dimensionless particle velocity $=v_r/W$, v_z/W
V Mean velocity of flow in sampling tube
W Free stream velocity
α Impaction parameter
δ Edge thickness of a tapered probe
η_a Inertial parameter for aspiration
η_p Inertial parameter for penetration
η_l Inertial parameter for loss
ρ Fluid density
ρ_p Particle density
τ Particle relaxation time
μ Fluid viscosity

INTRODUCTION

Numerous attempts have been made to investigate errors in sampling when aerosol particles are aspirated from a flowing gas stream into a sampling tube. The early studies were

primarily experimental in nature (Fahrenbach, 1931; Zimmerman, 1931) and the authors concluded that when the mean suction velocity, V, in the tube is not equal to the free stream velocity, W, the mean particle concentration in the sampling tube, C_i, will differ from that in the free stream, C_f. Subsequently, May and Druett (1953), Hains and Hemeon (1954) as well as Willcox (1957) found that the concentration ratio, C_i/C_f, which is also referred to as the aspiration coefficient, A, is not only a function of the velocity ratio W/V, but also dependent upon the dimensionless Stokes number, St

$$\mathrm{St}=\frac{\tau W}{d_i}, \tag{1}$$

where

$$\tau=\frac{\rho_p D_p^2 C}{18\mu} \tag{2}$$

is the particle relaxation time. However, their experimental data scattered greatly. The exact functional relationship between the aspiration coefficient and the Stokes number was not established.

Based on the theoretical consideration and experimental work, Badzioch (1959) (also see Davies, 1968; Zenker, 1971) derived a general form of the equation describing aspiration errors as follows,

$$A=1+\alpha(W/V-1), \tag{3}$$

where α is an impaction parameter depending on the Stokes number and other factors. Belyaev and Levin (1972) photographed particles during their entry into a sampling probe using flash illumination, and obtained results with considerably less scatter than previous workers. They concluded that the previous scatter in data could be explained by the following factors: (1) particle deposition on inlet; (2) particle rebound; and (3) effects due to the use of a thick-walled sampling tube. The previous experiments certainly included effects of these parameters. By taking photographs of tracks of particles aspirated into the sampling tube, they attempted to eliminate the effects of particle rebound and particle deposition on the inlet. A well-known semi-empirical equation for calculating the aspiration coefficient, A, was established in their subsequent paper (Belyaev and Levin, 1974)

$$A=1+(W/V-1)\frac{2+0.617V/W}{2+0.617V/W+\mathrm{St}^{-1}}. \tag{4}$$

Belyaev and Levin emphasized that equation (3) is valid for thin-walled sampling only. By 'thin-walled sampling', it is meant that the relative wall thickness of the tube, $d_o/d_i<1.1$ or if $d_o/d_i>1.1$, the taper angle of the tube β must be $<15°$ and the relative edge thickness δ/d_i, <0.05. For all other values of δ/d_i and β at $d_o/d_i>1.1$, the effect of wall thickness must be considered.

Some investigators, such as Durham and Lundgren (1980), Davies and Subari (1982) and Vincent *et al.* (1986), studied the problem by taking into account the effects of the misalignment of the sampling tube with the gas flow direction. Empirical relationships were developed between the aspiration coefficient and the Stokes number for various angles of misalignment. Durham and Lundgren also analyzed the particle loss on the inner walls of the sampling probe, but no quantitative conclusions on the loss were reached. Okazaki and Willeke (1987b), and Okazaki *et al.* (1987a) developed a model to describe the inner wall loss with the inclusion of inertial and gravitational factors.

Effects of the bluntness of samplers on the sampling errors were also assessed by several investigators (Vincent and Gibson, 1981; Mark *et al.*, 1982; Vincent *et al.*, 1985; Chung and Ogden, 1986). In these studies, the particle losses on the external walls of blunt samplers were examined as a function of the velocity ratio, W/V, and the Stokes number. The particle blow-off from external walls was identified as a source of errors for the sampling of solid particles.

The first attempt at a quantitative numerical study of the problem was that of Vitols (1966) who first developed a numerical model for anisokinetic sampling in a potential flow around a circular probe. The flow was assumed to be ideal, incompressible and irrotational. His

solution was obtained using the stream function approach with consideration of the inertial mechanism only. Recently, Rader and Marple (1983, 1988) investigated the anisokinetic sampling in a viscous laminar flow using the finite difference method for solving the complete Navier–Stokes equation. The effects of wall thickness were also studied. Their results are in reasonable agreement with the experimental data obtained in a turbulent flow by other researchers. Some other investigators such as Shahnam and Jurewicz (1986) focused their attention on the effect of fluid turbulence on anisokinetic sampling. They failed to detect recirculation near the sampling inlet, however their results compare fairly well with the previous experimental data.

In the present study of anisokinetic sampling, our interest is not only in the aspiration coefficient but also in the particle loss inside the sampling tube. As mentioned earlier, particle loss on the inner wall was noticed by some investigators. In general, loss of particles on the inside wall surfaces can be due to inertial impaction, gravitational settling, Brownian diffusion, turbulent deposition and, in the case of charged particles, by image force attraction. In the present study, our focus is on loss due to inertial effects only.

THEORETICAL MODELING

A general procedure used in the present study is as follows. First, the flow field around the sampling tube is generated using a numerical simulation technique. The particle trajectory is then calculated using this simulated flow field. By determining the limiting, or critical particle trajectories, the aspiration coefficient, A, the penetration coefficient, P, and loss coefficient, L, which are parameters characterizing anisokinetic sampling, are derived. In all cases, the probe is assumed to be in the form of a thin-walled circular tube aligned with and facing the flow.

Modeling approach for the flow field

For the circular sampling probe considered in the present study, the flow is rotationally symmetric about the centerline of the probe. Further, we assume that the flow is steady and incompressible, the fluid properties are constant, and there is no body force acting on the fluid. The following governing equations can be written for the flow in cylindrical coordinates:

$$\rho\left[u_r\frac{\partial u_r}{\partial r}+u_z\frac{\partial u_r}{\partial z}\right]=-\frac{\partial p}{\partial r}+\mu\left[\frac{\partial^2 u_r}{\partial r^2}+\frac{1}{r}\frac{\partial u_r}{\partial r}-\frac{u_r}{r^2}+\frac{\partial^2 u_r}{\partial z^2}\right] \tag{5}$$

$$\rho\left[u_r\frac{\partial u_z}{\partial r}+u_z\frac{\partial u_z}{\partial z}\right]=-\frac{\partial p}{\partial z}+\mu\left[\frac{\partial^2 u_z}{\partial r^2}+\frac{1}{r}\frac{\partial u_z}{\partial r}+\frac{\partial^2 u_z}{\partial z^2}\right] \tag{6}$$

and

$$\frac{\partial u_r}{\partial r}+\frac{u_r}{r}+\frac{\partial u_z}{\partial z}=0. \tag{7}$$

Equations (5) and (6) are the momentum equations, or the Navier–Stokes equations, and equation (7) is the continuity equation.

The fluid is then divided into a finite number of control volumes, and the discretized governing equations are written for each control volume. The velocity components and pressure at each node of the control volume are thus directly calculated. The detailed derivation is given by Patankar (1979). A computer code called SIMPLE (Semi-Implicit, Pressure-Linked Equations) has been developed by Patankar, which is the basic code used in the present study for solving the flow field. The discretized governing equations are solved in a calculation domain shown in Fig. 1 where the z-axis is located along the centerline of the tube. The radius of the calculation domain, R, was generally set to $10R_i$, except at high V/W ratios, where a larger value of R was used so that 5% of the total flow in the calculation domain was drawn into the sampling tube. This insured that the sampling flow into the sampling tube did not affect the free-stream boundary conditions used in the calculation.

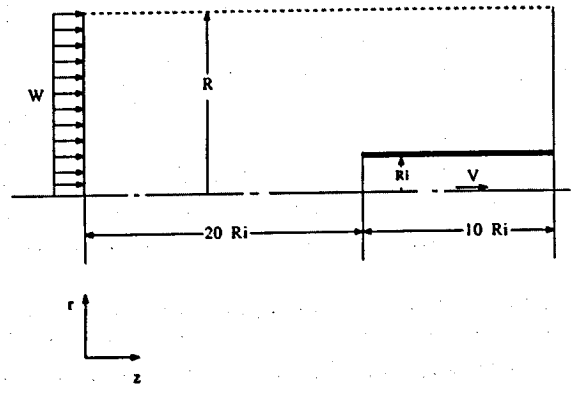

Fig. 1. Calculation domain used in numerical solutions.

More exactly, the boundary conditions used are:

(i) outer boundary, $r=R$: $u_z=W$, $u_r=0$

(ii) inlet, $z=0$: $u_z=W$, $u_r=0$

(iii) outlet, $z=Z_1$: for $0<r<R_i$, mean outflow velocity $=V$

(iv) tube axis, $r=0$: $\dfrac{\partial u_z}{\partial r}=0.$

The computation domain was divided into a finite number of control volumes by 32 grid lines in the z-direction and 36 grid lines in the r-direction. The grid spacing was finer near the walls and coarser away from the walls, increasing by factors of 1.1 in both z- and r-directions.

Calculation of the particle trajectories

Once the flow field is generated, the particle trajectories can be calculated using a numerical approach. The method is similar to that used by Marple (1970) and involves calculating the particle trajectory by integrating the equations of particle motion:

$$m\frac{dv_r}{dt}=F_{dr} \tag{8}$$

$$m\frac{dv_z}{dz}=F_{dz} \tag{9}$$

by means of the Runge–Kutta method, where v_r and v_z are the particle velocities in the r- and z-directions, and F_{dr} and F_{dz} are the corresponding fluid drag on the particles, the gravitational force on the particles having been neglected.

When a particle is moving at a constant velocity and at a low local Reynolds number, the Stokes drag is valid and can be applied. On the other hand, the Stokes drag law becomes invalid when $\mathrm{Re}_p>1$. An empirical drag law valid for the ultra-Stokesian regime can be used. The dimensionless equations of motion (see Friedlander, 1977; Rader and Marple, 1988) incorporating the experimental drag coefficient, C_D and the particle Reynolds number, Re_p, are:

$$\mathrm{St}\frac{dv'_r}{dt}=\frac{C_D\mathrm{Re}_p}{24}(u'_r-v'_r) \tag{10}$$

$$\mathrm{St}\frac{dv'_z}{dt}=\frac{C_D\mathrm{Re}_p}{24}(u'_z-v'_z), \tag{11}$$

where Re_p is the local particle Reynolds number given by

$$Re_p = Re_{p'w}[(u_r' - v_r')^2 + (u_z - v_z')^2]^{1/2} \tag{12}$$

and $Re_{p'w}$ is the particle Reynolds number based on the free stream gas velocity, W.

$$Re_{p'w} = \frac{\rho D_p W}{\mu}. \tag{13}$$

The empirical correlation between C_D and Re_p proposed by Sartor and Abbott (1975), and Serafini (1954) are used:

$$C_D = \frac{24}{Re_p}(1 + 0.0916\, Re_p) \qquad Re_p < 5 \tag{14}$$

$$C_D = \frac{24}{Re_p}(1 + 0.158\, Re_p^{2/3}) \qquad 5 < Re_p < 1000 \tag{15}$$

Definition of aspiration, penetration, and loss coefficients

As shown in Fig. 2, the aspiration coefficient, A, which characterizes the sampling error due to particle inertia, is defined as the ratio of aerosol concentration in the sampling inlet to that in the free stream.

$$A = \frac{C_i}{C_f}. \tag{16}$$

By defining a limiting particle trajectory as the trajectory dividing those particles that enter the sampling probe from those that do not, and assuming non-interaction among particles, the conservation equation for aerosols can be written as,

$$\int_0^{S_f} C_f w\, ds = \int_0^{S_i} C_i v\, ds, \tag{17}$$

where S_f is the cross-sectional area of stream tube formed by the limiting particle trajectories in the far upstream side of the sampling inlet, and S_i is the cross-sectional area of the sampling probe. Further, the aerosol concentration profile was assumed to be uniform at the inlet to the computation domain. The aspiration coefficient was then determined by combining equations (16) and (17),

$$A = \left(\frac{d'}{d_i}\right)^2 \frac{W}{V}. \tag{18}$$

Similarly, as shown in Fig. 3, the penetration coefficient is defined as the ratio of the particle concentration at the tube exit to that in the undisturbed free stream. The limiting trajectory

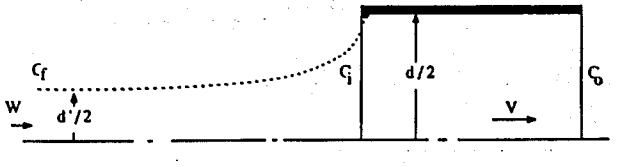

Fig. 2. Schematic of the limiting particle trajectory defining the aspiration coefficient.

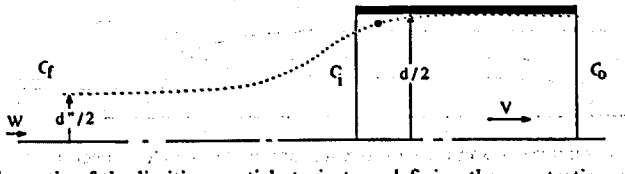

Fig. 3. Schematic of the limiting particle trajectory defining the penetration coefficient.

of the particles penetrating through the inlet then divides the particles that are collected by impaction on the tube wall from those that do not. The penetration coefficient is seen to be given by

$$P=\left(\frac{d''}{d_i}\right)^2\frac{W}{V}. \tag{19}$$

Finally, the fraction of particles that are lost by impaction, or the loss coefficient, L, can be found by difference,

$$L=A-P. \tag{20}$$

It is assumed in equation (19) that particles coming in contact with tube wall are removed by impaction and that particle rebound does not occur.

RESULTS

Figures 4 and 5 illustrate the streamlines and particle trajectories of the typical solutions for the case of sub-isokinetic ($V<W$) sampling and super-isokinetic ($V>W$) sampling, respectively. As the fluid undergoes changes in direction in the vicinity of the sampling inlet, the particles undergo similar changes in direction. However, due to particle inertia, the motion of the particle lags behind the fluid motion and it is this lag in particle motion that causes the anisokinetic sampling error to develop.

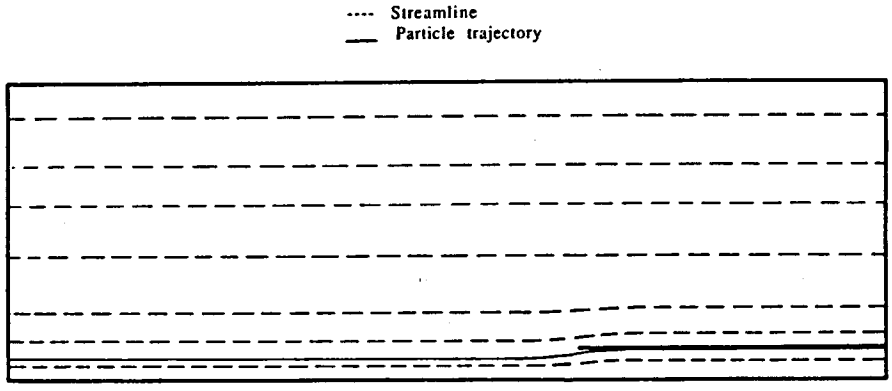

Fig. 4. A typical numerical solution of streamlines and particle trajectory in sub-isokinetic sampling (Re = 1000, $W/V = 2$).

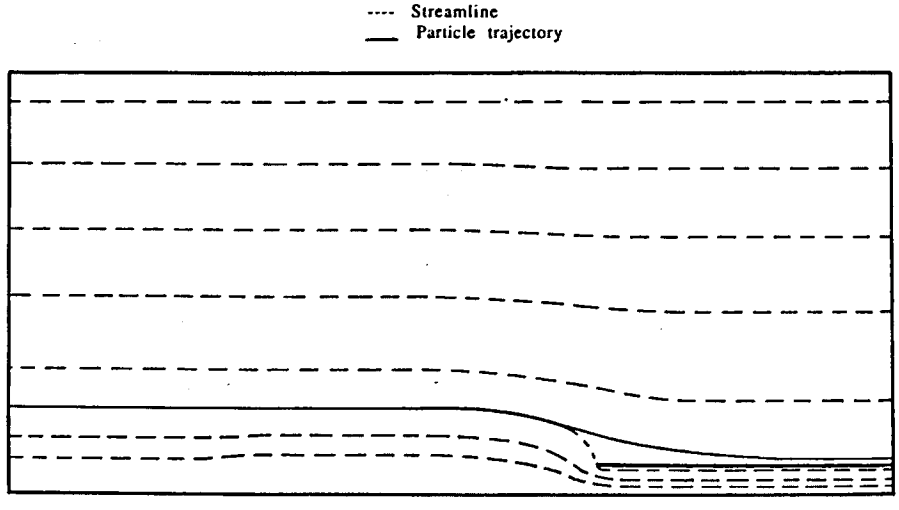

Fig. 5. A typical numerical solution of streamlines and particle trajectory in super-isokinetic sampling (Re = 1000, $W/V = 0.1$).

In the numerical modeling, although the particle motion could be simulated using the actual ultra-Stokesian drag law, equations (14) and (15), it was decided to carry out a baseline study where the Stokes law, $C_D = 24/\mathrm{Re}_p$, is assumed to be valid. Calculations were then made to determine to what extent departure from Stokes law would cause differences in the calculation results. Table 1 shows the calculated aspiration coefficient and penetration coefficient for the case of particle drag given by the Stokes law and that given by the actual ultra-Stokesian law. The difference is seen to be quite small for both small (<0.1) and large (>10) Stokes numbers, the greatest difference being about 7%, which occurs at a Stokes number of 1.0 and velocity ratios W/V of 0.1 and 10. Therefore, as a baseline study, it was decided to carry out all subsequent numerical calculations using the Stokes law.

For each given set of conditions, the aspiration and penetration coefficients were evaluated at 13 values of the Stokes number. Based on our preliminary numerical investigation and the experience of other researchers (Rader and Marple, 1988), it has been found that the aspiration coefficient has only a slight dependence on Reynolds numbers when the latter is not too small. Therefore, our calculation was made with a Reynolds number for the sampling tube, $\mathrm{Re} = \rho d_i W/\mu = 1000$, where the effect due to the variation of Reynolds number is expected to be small.

The aspiration, penetration and loss coefficients, A, P, and L, were determined using the method discussed above. In order to generalize the calculation results, it was decided to make use of the similarity between the inertial sampling errors and the mechanism of inertial impaction of particles. This similarity can be understood by viewing the schematic streamlines at the entrance to the sampling tube as shown in Fig. 6. As the velocity ratio

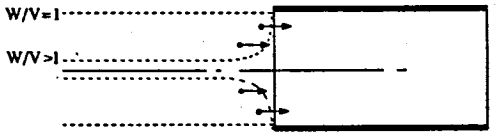

Fig. 6. Schematic streamlines and particle trajectories showing impaction of particles into void space causing enhanced particle collection in the sampled stream ($A>1$).

Table 1. Effects of ultra-Stokesian drag on aspiration and penetration coefficients*

	Aspiration coefficient, A					
	$W/V=2$		$W/V=5$		$W/V=10$	
St	Stokes	Ultra	Stokes	Ultra	Stokes	Ultra
0.01	1.019	1.020	1.086	1.080	1.211	1.202
0.1	1.167	1.142	1.705	1.689	2.630	2.521
1.0	1.685	1.615	3.755	3.590	7.315	6.847
10	1.936	1.865	4.902	4.700	9.565	9.402
100	2.047	1.989	5.023	4.981	10.19	10.05
	$W/V=0.5$		$W/V=0.2$		$W/V=0.1$	
St	Stokes	Ultra	Stokes	Ultra	Stokes	Ultra
0.01	0.990	0.991	0.968	0.970	0.934	0.947
0.1	0.911	0.927	0.766	0.789	0.648	0.682
1.0	0.640	0.662	0.343	0.356	0.213	0.227
10	0.532	0.545	0.216	0.224	0.110	0.118
100	0.505	0.510	0.204	0.209	0.100	0.104
	Penetration coefficient, A					
	$W/V=2$		$W/V=5$		$W/V=10$	
St	Stokes	Ultra	Stokes	Ultra	Stokes	Ultra
0.01	1.013	1.004	1.048	1.037	1.092	1.083
0.1	1.077	1.036	1.321	1.264	1.685	1.588
1.0	1.285	1.232	2.213	2.107	3.580	3.341
10	1.645	1.580	3.689	3.541	6.593	6.343
100	1.891	1.879	4.667	4.600	9.122	9.104

*Stokes = Stokes drag, Ultra = ultra-Stokesian drag, St = Stokes number $= \tau W/d_i$.

W/V varies from one to infinity (sub-isokinetic sampling), the diameter of the stream tube entering the sampling tube will decrease from d_i—the sampling tube diameter—to zero. Since some of the particles outside this stream tube can also enter the sampling tube by virtue of their inertia, the situation is similar to that of inertial impaction of particles into the void space of a virtual impactor. Since the performance of a virtual impactor can be described by means of an impactor efficiency, the inertia effect in anisokinetic sampling can also be described by an analogous parameter,

$$\eta_a = \frac{A-1}{W/V-1} \tag{21}$$

which will be referred to as the inertial parameter for aspiration.

From what is known about virtual impaction, one would expect this inertial parameter to have values ranging from 0 to 1 and that it would depend primarily on the Stokes number. Similarly, one can define an inertial parameter for penetration

$$\eta_p = \frac{P-1}{W/V-1}. \tag{22}$$

The difference between η_a and η_p then becomes the inertial parameter for particle loss,

$$\eta_l = \frac{A-P}{W/V-1}. \tag{23}$$

Figure 7 shows the values of η_a calculated by the numerical simulation procedure described above for the case of sub-isokinetic sampling ($W > V$) and correlated to the Stokes number for various values of W/V. Also shown for comparison are the values of η_a calculated from Balyaev and Levin's (1974) experimentally based equation. The agreement between the theory and experiment is seen to be quite good and both show that η_a can be correlated with Stokes number by a single function which is relatively independent of the value of W/V. The following equation has been fitted to the numerically generated functional relationship between η_a and St,

$$\eta_a = \frac{1}{1+0.418\,\mathrm{St}^{-1}} \tag{24}$$

which can be used for practical applications.

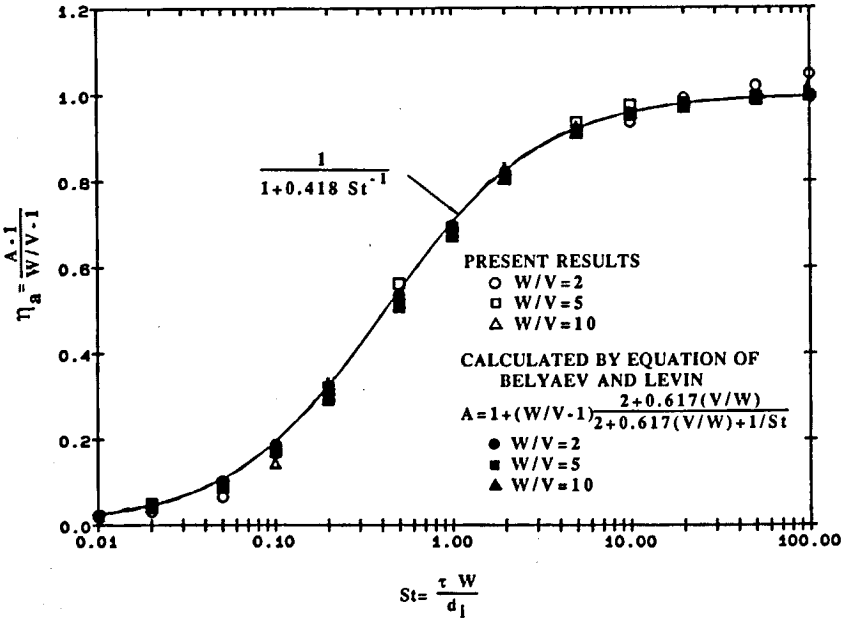

Fig. 7. Inertial parameter for aspiration, η_a, in sub-isokinetic sampling: comparisons with Belyaev and Levin's results for $W/V = 2.5$ and 10.

In the case of super-isokinetic sampling ($V > W$), it was found that the inertial parameter for aspiration, η_a, can be correlated with the parameter $\mathrm{St}(V/W)^{1/2}$. This correlation is shown in Fig. 8 along with that based on Belyaev and Levin's empirically-based predictions. Again, the numerical results are found to be in good agreement with the experimentally based results. Further, both results show that η_a is uniquely related to the parameter $\mathrm{St}(V/W)^{1/2}$. A least square fit of the numerically generated results gives the following equation,

$$\eta_a = \frac{1}{1+0.506(\mathrm{St}\sqrt{V/W})^{-1}}. \tag{25}$$

Combining equations (24) and (25) we have,

$$\eta_a = \begin{cases} \dfrac{1}{1+0.418\,\mathrm{St}^{-1}} & W/V > 1 \\ \dfrac{1}{1+0.506(\mathrm{St}\sqrt{V/W})^{-1}} & W/V < 1. \end{cases} \tag{26}$$

The results for the inertial parameters for penetration and particle loss, η_p and η_l are shown in Figs 9 and 10. The corresponding empirical fitting equations are

$$\eta_p = \frac{1}{1+2.66\,\mathrm{St}^{-2/3}} \qquad W/V > 1 \tag{27}$$

$$\eta_l = \frac{1}{1+0.418\,\mathrm{St}^{-1}} - \frac{1}{1+2.66\,\mathrm{St}^{-2/3}} \qquad W/V > 1. \tag{28}$$

For $W/V < 1$, particle impaction occurs on the external surface of the sampling tube only, in which case, $A = P$ and $L = 0$.

From Fig. 10, one can see that the maximum loss due to the inertial impaction occurs at a Stokes number of about one. Based on the experimental data, Durham and Lundgren (1980) qualitatively observed that the particle loss in the tube increased with particle size and decreased with increasing the tube diameter. In other words, the loss increased with increasing Stokes number. Our present study indicates that if only the inertial impaction mechanism is included, particle loss in the inner wall will not simply increase with Stokes

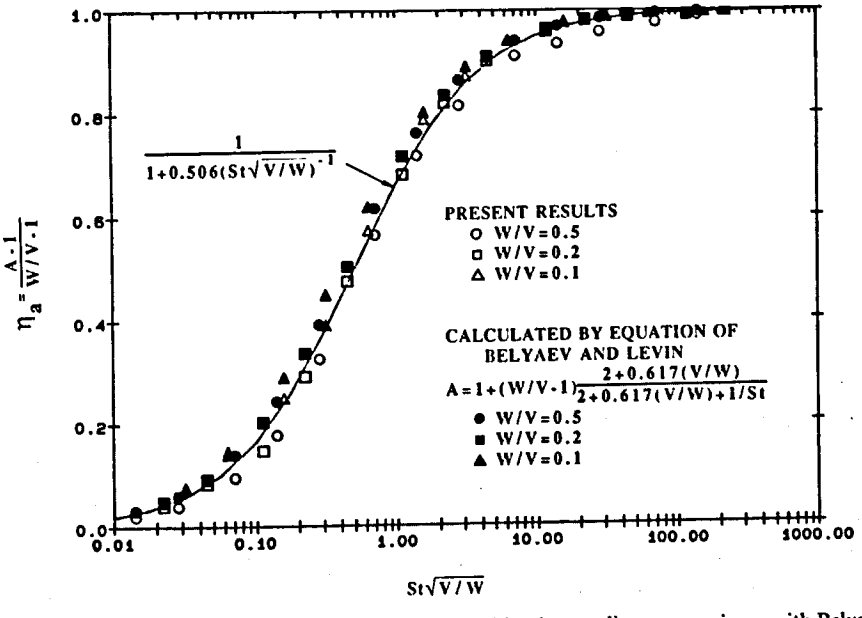

Fig. 8. Inertial parameter for aspiration, η_a, in super-isokinetic sampling: comparisons with Belyaev and Levin's results for $W/V = 0.5$, 0.2 and 0.1.

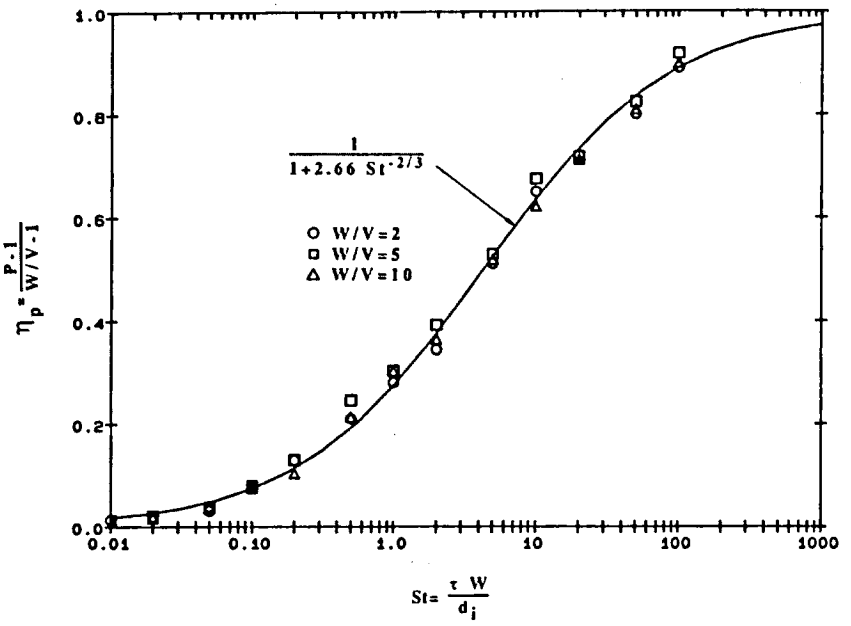

Fig. 9. Inertial parameter for penetration, η_p, for $W/V=2$, 5 and 10.

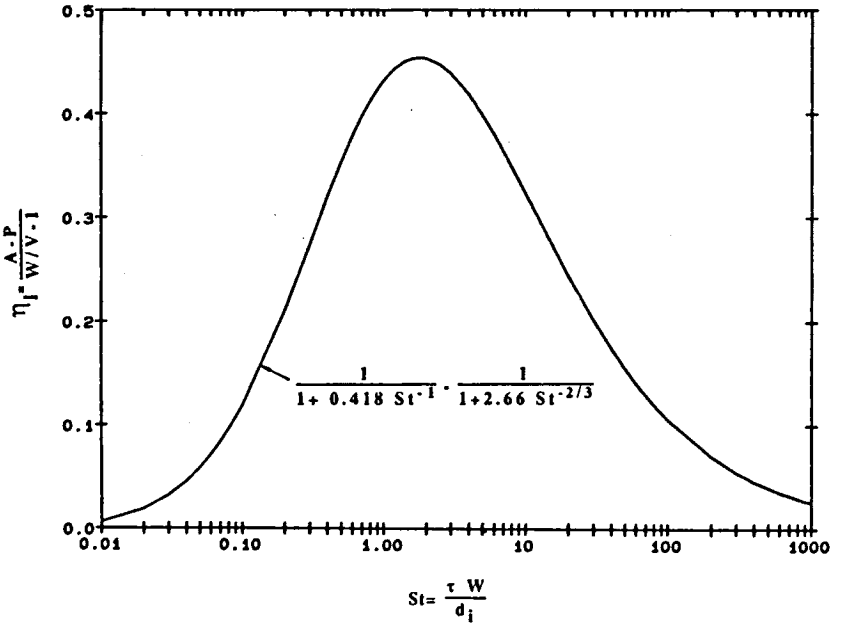

Fig. 10. Inertial parameter for loss, η_I, in sub-isokinetic sampling ($V < W$).

number—it first increases with increasing Stokes number, reaching a peak at a Stokes number of around one; thereafter, it decreases with further increase in the Stokes number. This can be explained as follows. At St = 0, impaction losses inside the sampling tube will not occur, i.e. $L=0$, since particles without inertia will follow the streamlines completely. On the other hand, particles with very large inertia, i.e. St = ∞, would travel in a straight path regardless of the deflection of streamlines near the sampling inlet, in which case equations (18) and (19) show that $A=P=W/V$ or $L=0$. Therefore, the maximum particle loss by impaction is expected to occur at an intermediate Stokes number, which has been found to be in the vicinity of St = 1.0. If the gravitational settling is included in the loss in the case of a

horizontal sampling tube, it can be expected that gravitational settling will dominate the loss when the Stokes number becomes large.

Equations (26) and (27) can be rearranged as follows to give the aspiration and penetration coefficients directly

$$A=\begin{cases}1+(W/V-1)\dfrac{1}{1+0.418\,\mathrm{St}^{-1}} & W/V>1\\[2ex] 1+(W/V-1)\dfrac{1}{1+0.506(W/V)^{1/2}\mathrm{St}^{-1}} & W/V<1;\end{cases} \tag{29}$$

$$P=\begin{cases}1+(W/V-1)\dfrac{1}{1+2.66\,\mathrm{St}^{-2/3}} & W/V>1\\[2ex] 1+(W/V-1)\dfrac{1}{1+0.506(W/V)^{1/2}\mathrm{St}^{-1}} & W/V<1.\end{cases} \tag{30}$$

Table 2. Aspiration coefficients, A_c and A_f, obtained from the numerical solution and the fitting equation ($\mathrm{St}=\tau W/d_i$ = Stokes number)

(a) Sub-isokinetic sampling

$$A_f=1+(W/V-1)\frac{1}{1+0.418\,\mathrm{St}^{-1}}$$

St	A_c	A_f	A_c	A_f	A_c	A_f
	$W/V=2$		$W/V=5$		$W/V=10$	
0.01	1.019	1.023	1.086	1.093	1.211	1.210
0.02	1.031	1.045	1.200	1.182	1.440	1.412
0.05	1.066	1.106	1.372	1.420	1.864	1.961
0.1	1.167	1.193	1.705	1.702	2.630	2.731
0.2	1.325	1.323	2.284	2.294	3.982	3.912
0.5	1.534	1.542	3.250	3.178	5.746	5.910
1.0	1.685	1.705	3.755	3.820	7.315	7.346
2.0	1.805	1.827	4.226	4.308	8.464	8.444
5.0	1.913	1.922	4.743	4.691	9.334	9.305
10	1.936	1.959	4.902	4.839	9.565	9.638
20	1.992	1.979	4.922	4.918	9.741	9.815
50	2.021	1.991	4.976	4.966	9.876	9.925
100	2.047	1.996	5.023	4.983	10.19	9.965
Mean deviation (%)		1.34		1.42		1.92

(b) Super-isokinetic sampling

$$A_f=1+(W/V-1)\frac{1}{1+0.506(W/V)^{1/2}\,\mathrm{St}^{-1}}$$

St	A_c	A_f	A_c	A_f	A_c	A_f
	$W/V=0.5$		$W/V=0.2$		$W/V=0.1$	
0.01	0.990	0.984	0.968	0.966	0.934	0.947
0.02	0.983	0.973	0.933	0.935	0.867	0.900
0.05	0.952	0.938	0.882	0.855	0.775	0.785
0.1	0.911	0.890	0.766	0.754	0.648	0.653
0.2	0.837	0.822	0.619	0.624	0.487	0.500
0.5	0.717	0.708	0.452	0.449	0.306	0.318
1.0	0.640	0.642	0.343	0.347	0.213	0.224
2.0	0.592	0.578	0.278	0.281	0.159	0.166
5.0	0.544	0.533	0.233	0.234	0.122	0.127
10	0.532	0.517	0.216	0.217	0.110	0.114
20	0.521	0.508	0.210	0.208	0.105	0.107
50	0.512	0.503	0.207	0.203	0.102	0.103
100	0.505	0.501	0.204	0.201	0.100	0.101
Mean deviation (%)		1.62		1.07		2.94

The values given by equations (29) and (30) and those obtained directly from the numerical solutions are tabulated and compared in Tables 2 and 3. The mean deviation of the calculated data from the fitting equations is quite small, indicating that the fitting equations represent the calculated numerical results quite well. The comparison of the numerical solution with Belyaev and Levin's empirical data is shown in Fig. 11. They are in very good agreement with each other for $0.2 < W/V < 5$. However, the discrepancy becomes somewhat larger when the velocity ratio is higher or lower. The cause of the discrepancy may be due to the ultra-Stokesian effects and the fact that the very high or low velocity ratio is beyond the applicable range of the Belyaev and Levin's empirically based formula.

The penetration coefficient, P, is plotted as a function of Stokes number at various velocity ratios in Fig. 12. In Fig. 13 the relationship between the loss coefficient and the Stokes

Table 3. Penetration coefficients, P_c and P_f, obtained from numerical solutions and the fitting equation

$$\left(\mathrm{St}=\frac{\tau W}{d_i}=\text{Stokes number};\ P_f=1+(W/V-1)\frac{1}{1+2.66\,\mathrm{St}^{-2/3}}\right)$$

St	P_c	P_f	P_c	P_f	P_c	P_f
	$W/V=2$		$W/V=5$		$W/V=10$	
0.01	1.013	1.017	1.048	1.068	1.092	1.154
0.02	1.021	1.027	1.085	1.107	1.156	1.242
0.05	1.031	1.048	1.152	1.194	1.369	1.437
0.1	1.077	1.075	1.321	1.399	1.685	1.674
0.2	1.132	1.114	1.523	1.456	1.936	2.025
0.5	1.212	1.191	1.879	1.765	2.876	2.723
1.0	1.285	1.273	2.213	2.092	3.580	3.459
2.0	1.344	1.373	2.567	2.494	4.277	4.363
5.0	1.508	1.523	3.115	3.094	5.665	5.712
10	1.645	1.635	3.698	3.542	6.593	6.712
20	1.722	1.734	3.871	3.939	7.413	7.612
50	1.800	1.836	4.297	4.344	8.292	8.525
100	1.891	1.890	4.667	4.560	9.122	9.011
Mean deviation (%)		1.03		2.93		3.37

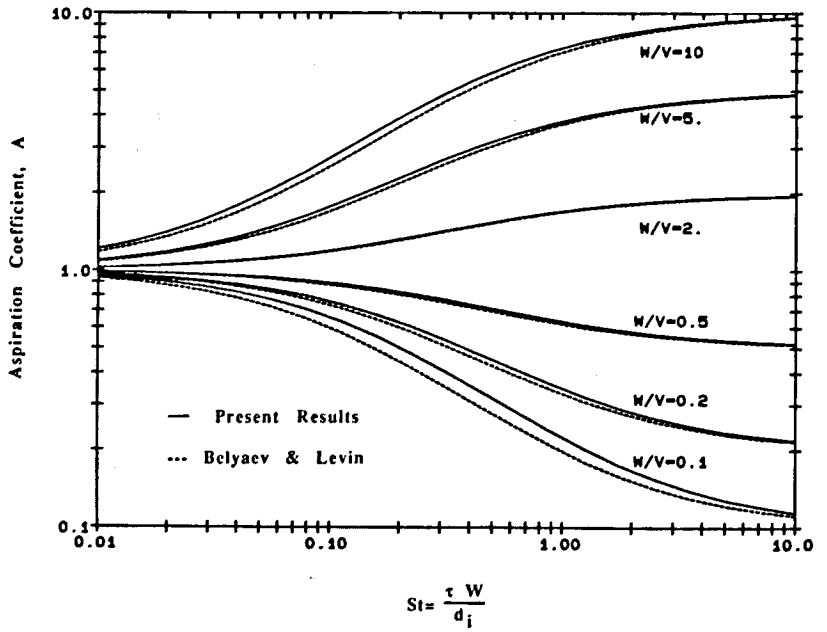

Fig. 11. Comparisons of the present results for aspiration coefficient with Belyaev and Levin's results.

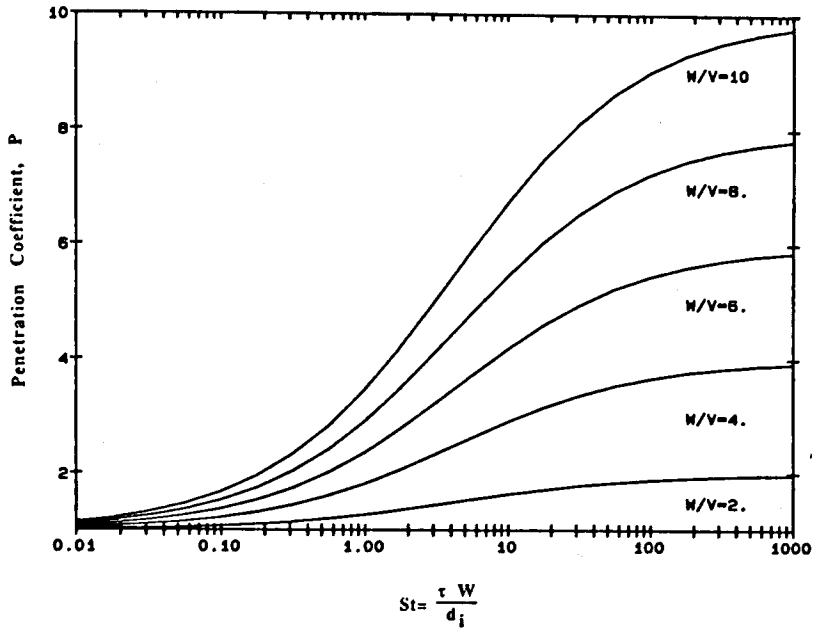

Fig. 12. Penetration coefficient for sub-isokinetic sampling ($V < W$).

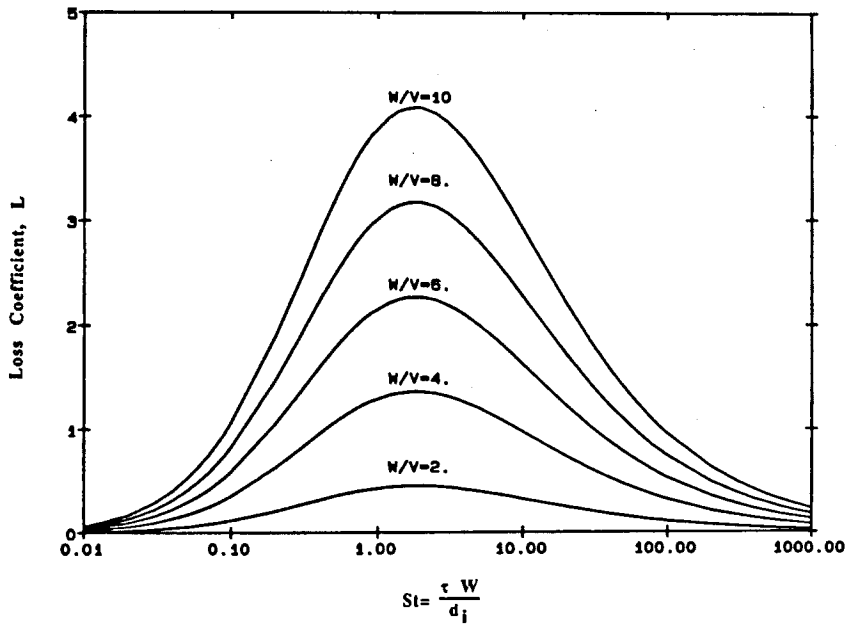

Fig. 13. Loss coefficient for sub-isokinetic sampling at various velocity ratios.

number is plotted with the velocity ratio shown as a parameter. From these two figures, it is concluded that the absolute particle loss increases with increasing velocity ratio.

CONCLUSIONS

In the present study, the nature of the anisokinetic sampling process has been successfully characterized by means of a numerical simulation technique based on the method of computational fluid mechanics. Equations relating the Stokes numbers to the inertial parameters for aspiration, penetration and loss have been established. In the case of super-isokinetic sampling, the inertial parameter for aspiration has been found to be uniquely

related to the parameter St $(V/W)^{1/2}$. The particle loss on the tube wall due to inertial impaction, was established quantitatively. The numerical results for the aspiration coefficient have been found to agree with the classical Balyaev and Levin results for velocity ratios W/V between 0.2 and 5. Beyond this range, the results obtained by the present numerical simulation technique are believed to be more accurate. Therefore, more accurate predictions can be made with the present results for higher and lower velocity ratios.

Acknowledgements—The authors gratefully acknowledge the financial support of the Particulate Contamination Control Research Consortium at the University of Minnesota. Members of the Consortium include Applied Materials, Inc., Control Data Corp., Donaldson Company, Inc., IBM Corporation, Millipore Corp., Nupro Company, Texas Instruments, Inc., and TSI, Inc.

REFERENCES

Badzioch, S. (1959) *Br. J. appl. Phys.* **10**, 26.
Belyaev, S. P. and Levin, L. M. (1972) *J. Aerosol Sci.* **3**, 127.
Belyaev, S. P. and Levin, L. M. (1974) *J. Aerosol Sci.* **5**, 325.
Chung, K. Y. K. and Ogden, T. L. (1986) *Aerosol Sci. Technol.* **5**, 81.
Davies, C. N. (1968) *Br. J. appl. Phys. (J. Phys. D)* **2**, 921.
Davies, C. N. and Subari, M. (1982) *J. Aerosol Sci.* **13**, 59.
Durham, M. D. and Lundgren, D. A. (1980) *J. Aerosol Sci.* **11**, 179.
Fahrenbach, W. (1931) *Forschung (Berlin)* **2**, 395.
Friedlander, S. K. (1977) *Smoke, Dust and Haze.* Wiley-Interscience, New York.
Hains, G. F. and Hemeon, W. C. L. (1954) *Air Repair* **4**, 159.
Mark, D., Vincent, J. H. and Witherspoon, W. A. (1982) *Aerosol Sci. Technol.* **1**, 463.
Marple, V. A. (1970) Ph.D. thesis, Mechanical Engineering Department, University of Minnesota, Minneapolis, Minnesota.
May, K. and Druett, H. (1953) *Br. J. ind. Med.* **10**, 142.
Okazaki, K., Wiener, R. W. and Willeke, K. (1987a) *Envir. Sci. Technol.* **21**, 178.
Okazaki, K. and Willeke, K. (1987b) *Aerosol Sci. Technol.* **7**, 275.
Patankar, S. V. (1979) *Numerical Heat Transfer and Fluid Flow.* McGraw-Hill-Hemisphere, New York.
Rader, D. J. and Marple, V. A. (1983) *Aerosol Sci. Technol.* **2**, 249.
Rader, D. J. and Marple, V. A. (1988) *Aerosol Sci. Technol.* **8**, 283.
Sartor, J. D. and Abbott, C. E. (1975) *J. appl. Meteorol.* **14**, 232.
Serafini, J. S. (1954) *NACA Report* 1159.
Shahnam, M. and Jurewich, J. T. (1986) Solid-gas flow. *Proceedings of the ASME/AIAA Thermophysics Conference*, p. 145.
Vincent, J. H., Emmett, P. C. and Mark, D. (1985) *Aerosol Sci. Technol.* **4**, 17.
Vincent, J. H. and Gibson, H. (1981) *Atmos. Envir.* **15**, 703.
Vincent, J. H., Stevens, D. C., Mark, D., Marshall, M. and Smith, T. A. (1986) *J. Aerosol Sci.* **17**, 211.
Vitols, V. (1966) *J. Air Pollut. Control Ass.* **16**, 79.
Willcox, J. D. (1957) Isokinetic flow and sampling of airborne particulates. In *Artificial Stimulation of Rain*, p. 177.
Zenker, P. (1971) *Staub-Reinhalt Luft* **31**, 30.
Zimmerman, E. L. (1931) *VDIZ* **75**, 481.